Molecular Therapy
Nucleic Acids
Original Article

Supercoiled DNA percentage: A key in-process control of linear DNA template for mRNA drug substance manufacturing

Xijun Piao,[1,2] Yujie Tang,[1,4] Xiuzhi Li,[1,4] Weicheng Zhang,[1,4] Wei Yang,[2] Xining Xu,[1] Wenjing Wang,[1,4] Jiajia Jiang,[1,4] Jun Xu,[1,4] Kunkun Hu,[2] Meiling Xu,[2] Mengjie Liu,[2] Mengfei Sun,[1,4] and Lin Jin[1,2,3,4]

[1]CATUG Biotechnology, Suzhou 215000, China; [2]Wuhan CATUG Biotechnology, Wuhan 430074, China; [3]CATUG Inc, Cambridge, MA 02141, United States; [4]CATUG Life Technology, Suzhou 215000, China

The development of messenger RNA (mRNA) vaccines and therapeutics necessitates the production of high-quality *in vitro*-transcribed mRNA drug substance with specific critical quality attributes (CQAs), which are closely tied to the uniformity of linear DNA template. The supercoiled plasmid DNA is the precursor to the linear DNA template, and the supercoiled DNA percentage is commonly regarded as a key in-process control (IPC) during the manufacturing of linear DNA template. In this study, we investigate the influence of supercoiled DNA percentage on key mRNA CQAs, including purity, capping efficiency, double-stranded RNA (dsRNA), and distribution of poly(A) tail. Our findings reveal a significant impact of supercoiled DNA percentage on mRNA purity and *in vitro* transcription yield. Notably, we observe that the impact on mRNA purity can be mitigated through oligo-dT chromatography, alleviating the tight range of DNA supercoiled percentage to some extent. Overall, this study provides valuable insights into IPC strategies for DNA template chemistry, manufacturing, and controls (CMC) and process development for mRNA drug substance.

INTRODUCTION

The COVID-19 pandemic has propelled the rapid development of mRNA vaccines and therapeutics, leading to an upsurge in mRNA pipelines across various stages of discovery research and clinical trials.[1,2] To support these efforts, the manufacturing of high-quality mRNA as drug substance is of utmost importance.[3,4] A functional mRNA structure comprises the 5′ cap, 5′ untranslated region (UTR), coding sequence (CDS), 3′ UTR, and 3′ poly(A) tail (Figure 1A). A typical mRNA manufacturing process begins with *in vitro* transcription (IVT), an enzymatic reaction that utilizes a linear DNA with bacteriophage promoter as the template for RNA synthesis.[5] Two widely accepted capping processes are employed to ensure correct cap structure at the 5′ end of the mRNA sequence: the classical capping process involving a separate post-IVT enzymatic step,[6] and the co-transcriptional process utilizing dinucleotide or trinucleotide cap analogues such as ARCA[7] and CleanCap AG[8] during a one-pot IVT reaction. In addition to the upstream IVT and capping reaction, the downstream purification process is crucial in mRNA drug substance manufacturing. Compared with lithium chloride (LiCl) precipitation,[9] which is a non-affinity purification method commonly used in research labs but challenging to scale up, oligo-dT chromatography that selectively binds the 3′ poly(A) tail of mRNA is a more effective and easily scaled-up affinity purification method to improve mRNA purity by removing tailless fragments.[10,11] LiCl precipitation represents a non-affinity purification method in our study. For buffer exchange and some impurity removal in a scaled-up production, tangential flow filtration (TFF) is often used instead of LiCl precipitation.[12,13]

DNA template, a pivotal starting material for mRNA IVT reaction, encodes nearly all the functional elements of mRNA, including 5′ UTR, CDS, 3′ UTR, and 3′ poly(A) tail. Although the 5′ cap is an enzymatically or chemically added structure in front of 5′ UTR and is not encoded in the DNA template, it may still be affected by the incomplete starting sequence of 5′ UTR. Consequently, understanding the correlation between DNA template quality and product-related CQAs is crucial for mRNA process development and manufacturing. These CQAs include mRNA purity (percentage of intact or full-length mRNA out of total RNA, or integrity), capping efficiency (percentage of correctly capped mRNA out of mRNA with intact 5′ end), poly(A) tail distribution, double-stranded RNA (dsRNA) content, as well as the potency (protein expression efficiency).[14] Note that dsRNA is an important RNA type and immunogenic byproduct formed during IVT reaction through various mechanisms,[15,16] and uncapped mRNA also possesses immunostimulatory properties.[17] The supercoiled plasmid DNA, serving as a precursor to the linear DNA template, plays a critical role in determining the homogeneity of the linear DNA template, with the supercoiled (SC) DNA percentage serving as a key in-process control (IPC) during process development and manufacturing. However, very limited studies have comprehensively explored the correlation between the supercoiled DNA percentage and CQAs of mRNA drug substances.

Herein, we present a study that investigates how the supercoiled plasmid DNA percentage affects the major CQAs of mRNA drug substance

Received 17 February 2024; accepted 16 May 2024;
https://doi.org/10.1016/j.omtn.2024.102223.

Correspondence: Lin Jin, CATUG Biotechnology, Suzhou 215000, China.
E-mail: lin.jin@catugbio.com

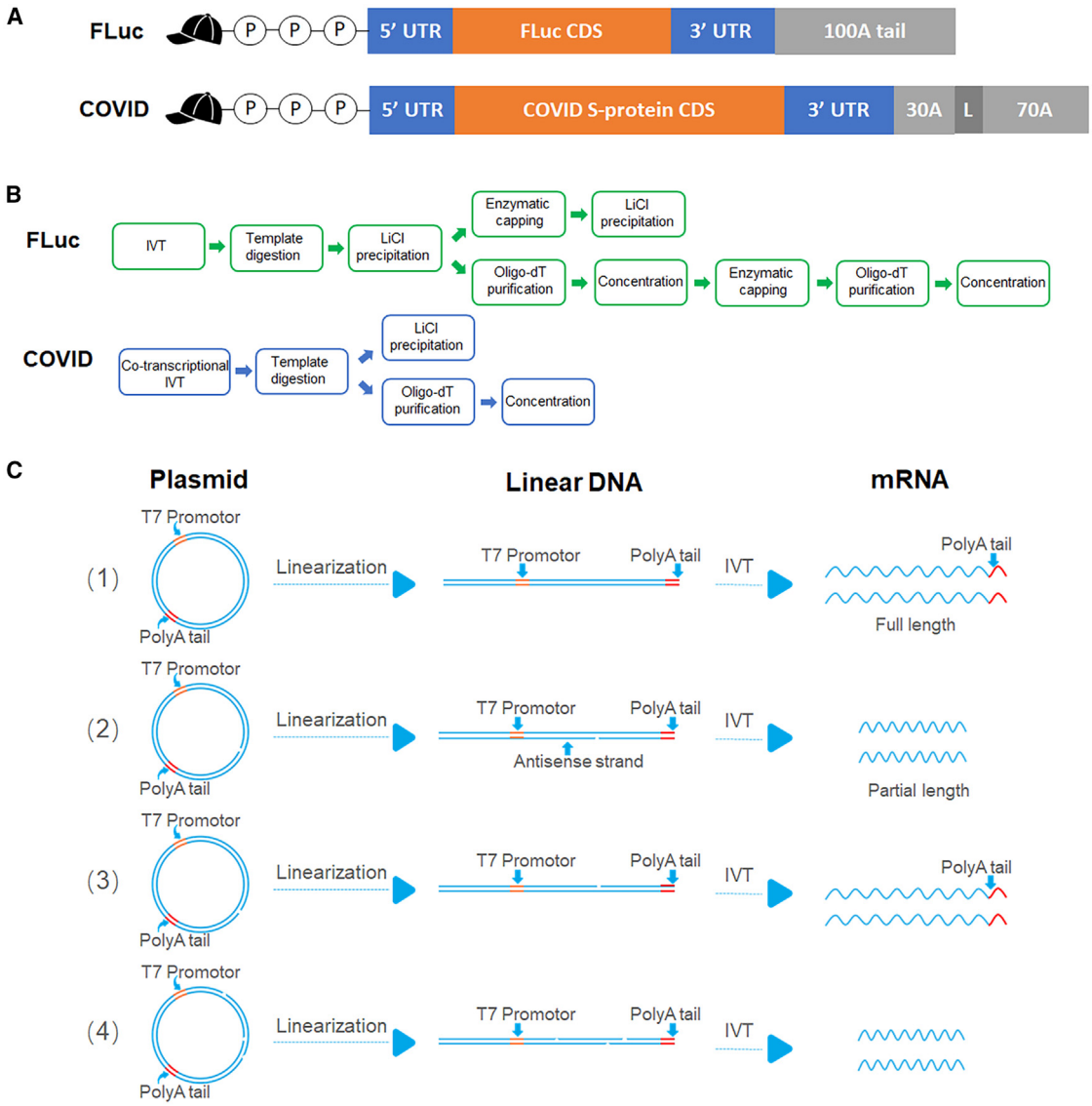

Figure 1. Illustration of mRNA structures, different mRNA manufacturing processes, and supercoiled DNA affecting mRNA purity

(A) Two mRNA structures with different poly(A) tails. L stands for a 10-nt non-full-A linker. (B) Four different mRNA manufacturing processes used in this study, including enzymatic capping, co-transcriptional capping, non-affinity purification, and affinity purification. (C) Lower supercoiled DNA generating heterogeneous linear DNA template, leading to mRNA of lower purity.

manufactured from four different processes, covering enzymatic capping and co-transcriptional capping as well as non-affinity purification and affinity purification. The findings contribute insights into an in-process control strategy for linear DNA template production and the determination of suitable processes for mRNA manufacturing.

RESULTS

Impact of supercoiled DNA percentage on mRNA purity and integrity

In our study, we employed firefly luciferase (FLuc) plasmid (Figure S1) and COVID-19 S-protein (COVID) plasmid (Figure S2) to serve as DNA templates for coding mRNAs. More specific, FLuc mRNA consists of about 2,000 nucleotides (nt), while COVID mRNA is about 4,000-nt in length. The poly(A) tail of FLuc mRNA is a continuous 100-nt poly A tail, whereas COVID mRNA is a segmented 100-nt poly(A) tail that has a short linker inserted between 30A and 70A (Figure 1A). FLuc mRNA with GG as starting sequence is suitable for enzymatic capping, while COVID mRNA starting with AG is better for co-transcriptional capping. Thus, we utilized different capping processes in the upstream for FLuc and COVID mRNA synthesis (Figure 1B) and also applied two kinds of purification processes in the downstream for comparison.

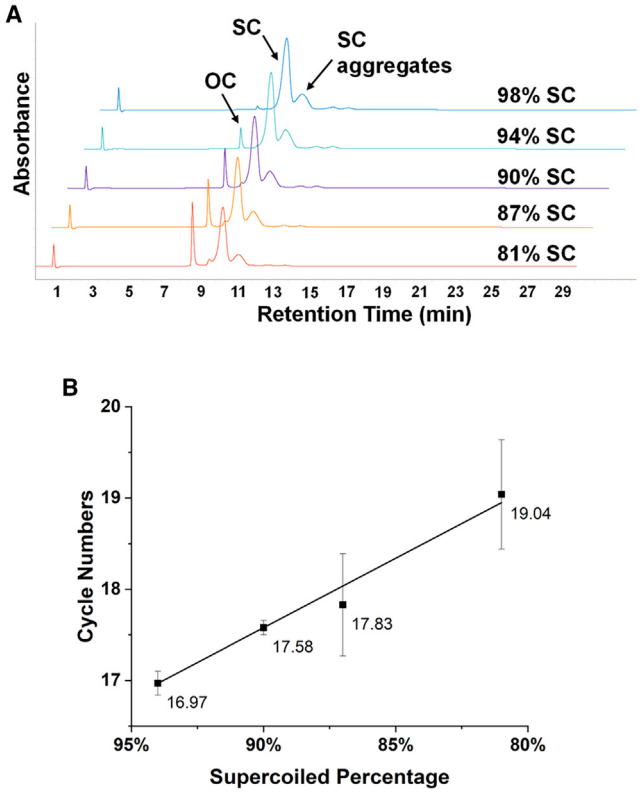

Figure 2. Changes of supercoiled DNA percentage on HPLC and heterogeneity of linear DNA template by qPCR

(A) Decreasing FLuc supercoiled (SC) DNA percentage and increasing open-circular (OC) DNA percentage with heat. (B) Increasing cycle numbers with more heterogeneous FLuc linear DNA template. Data are represented as mean ± SD.

Heat treatment on plasmid DNA is known to generate open-circular (OC) DNA[18] by creating nicks on random spots of any strand. These nicks will be further inherited by linear DNA templates that might potentially affect mRNA integrity (Figure 1C). Following the methods described in the "plasmids and DNA template generation" section, we were able to produce each plasmid DNA with target supercoiled percentages.

For the FLuc plasmid, the target supercoiled percentages were 100%, 95%, 90%, 85%, and 80%. In practice, we got FLuc plasmids with supercoiled percentages at 98%, 94%, 90%, 87%, and 81% (Table S1). Similarly, for the COVID plasmid, we got plasmids with supercoiled percentage at 96% 88%, 79%, 70%, and 59% after heat treatments to target 100%, 90%, 80%, 70%, and 60% by design (Table S2). The actual supercoiled DNA percentages were determined by the integration of high-pressure liquid chromatography (HPLC) peaks under absorbance at 260 nm, as shown in Figures 2A (FLuc) and S3 (COVID). An OC control was generated by a nicking endonuclease, Nt.BtsI, and confirmed the retention time of OC plasmid generated by heat on HPLC analysis (Figure S4). As expected, incubation at elevated temperatures and longer time resulted in an increase in nicks or OC plasmids, leading to a decrease in the supercoiled DNA percentage. Once the plasmids were linearized, we further analyzed the integrity of linear DNA templates by quantitative PCR (qPCR). The cycle numbers obtained from qPCR indicated how much amplification required to reach a certain cycle threshold (Ct). Theoretically, with more correct starting materials, it took fewer amplification cycles to reach a certain Ct. As shown in Figure 2B, linear DNA templates from plasmids of lower supercoiled percentages apparently required more amplification cycles, indicating these linear DNA templates were associated with reduced integrity due to a higher number of nicks.

We then proceeded to IVT synthesis of mRNA using linear DNA templates generated from plasmids of different supercoiled percentages. Capillary electrophoresis (CE) analysis of mRNAs generated through the non-affinity purification process revealed increasing shoulder peaks preceding the main peak, indicating a decrease in the percentage of full-length mRNA purity as the supercoiled percentage decreased (Figures 3A, 3C, S5, and S6). Since lower supercoiled percentage templates inherit more random nicks, RNA polymerase is not capable of reading through these nicks easily,[19] resulting in the generation of more mRNA fragments of varying shorter lengths instead of the intact mRNA. These mRNA fragments later contributed to the formation of broad shoulder peaks on CE. As the plasmid supercoiled percentage decreased, the corresponding mRNA purity continued to decline (Figures 3E and 3F). Notably, COVID mRNA appeared to be more affected by the supercoiled DNA percentage compared to FLuc mRNA. Even at a supercoiled DNA percentage of approximately 80%, significant differences in mRNA purity were observed (62% for FLuc mRNA vs. 21% for COVID mRNA). This observation might be attributed to the length of the target gene sequence. Specifically, the COVID sequence is approximately twice as long as the FLuc sequence, making it more susceptible to damage caused by heat, even at the same supercoiled DNA percentage.

Enhanced mRNA purity and reduction of supercoiled DNA impact through affinity purification

Oligo-dT chromatography is a widely utilized method in mRNA processes known for effectively removing degraded mRNA lacking a sufficient poly(A) tail. The principle behind this technique relies on the base pairing between adenine and thymine, enabling mRNA molecules with complete or partially intact poly(A) tails to be retained on the matrix. In contrast, mRNA fragments without a sufficient poly(A) tail are eliminated during the loading and washing steps.[11] However, it should be noted that degraded mRNA fragments with a poly(A) tail may not be separated. When oligo-dT chromatography was applied to both the FLuc and COVID mRNAs, a significant increase in mRNA purity was observed (Figures 3B, 3D, S7, and S8), mitigating the impact caused by low supercoiled DNA percentages initially.

As depicted in Figures 3E and 3F, the purity of FLuc mRNAs derived from different supercoiled percentages approached approximately

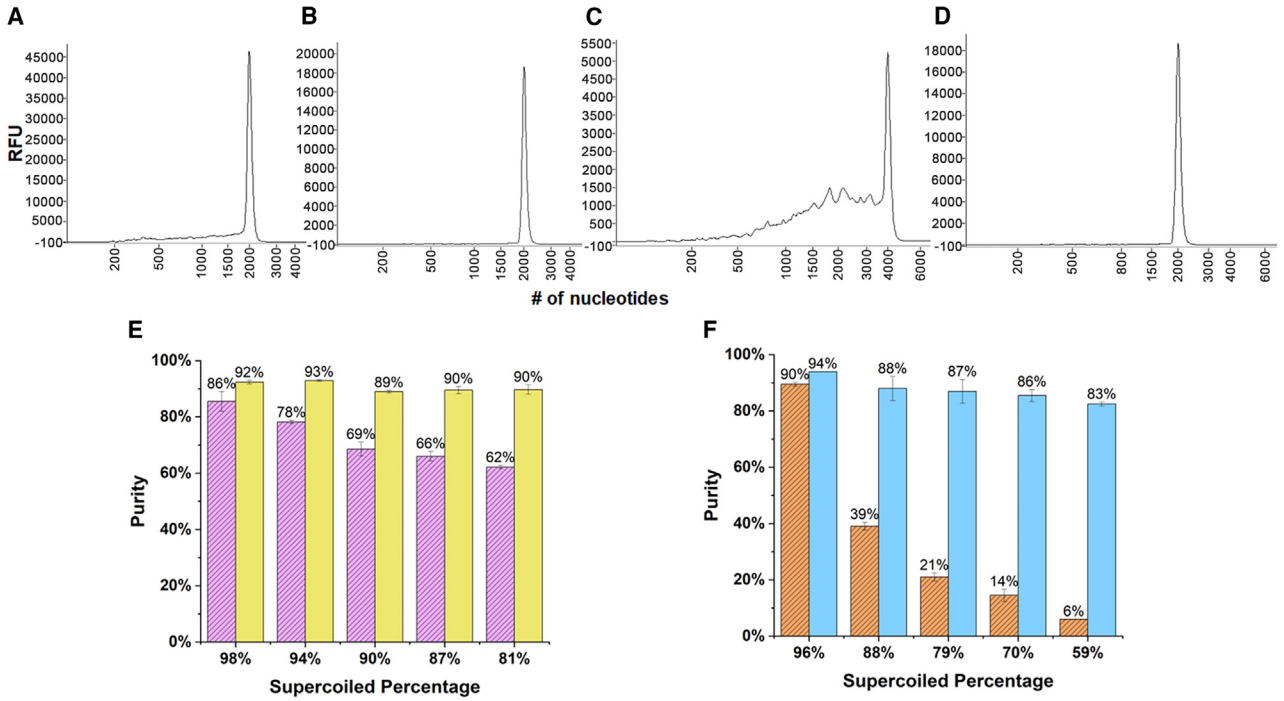

Figure 3. Comparison of mRNA purity

(A) FLuc mRNA purity from 80% supercoiled DNA and purified by LiCl precipitation. (B) FLuc mRNA purity from 80% supercoiled DNA and purified by oligo-dT chromatography. (C) COVID mRNA purity from 80% supercoiled DNA and purified by LiCl precipitation. (D) COVID mRNA purity from 80% supercoiled DNA and purified by oligo-dT chromatography. Full chromatograms can be found in Figures S5–S8. (E) FLuc mRNA purity change with different supercoiled DNA percentage (purple is FLuc mRNA manufactured by LiCl precipitation and yellow is FLuc mRNA manufactured by oligo-dT chromatography). (F) COVID mRNA purity change with different supercoiled DNA percentage (orange is COVID mRNA manufactured by LiCl precipitation and blue is COVID mRNA manufactured by oligo-dT chromatography). Data are represented as mean ± SD.

90% after undergoing oligo-dT chromatography. Similarly, COVID mRNA purity was raised to at least 83% from its initial lowest value of only 6%. Notably, the FLuc mRNAs were produced through enzymatic capping process and coupled with affinity purification including two oligo-dT steps. This purification process resulted in remarkable consistency in high mRNA purity across all the groups, regardless of initial supercoiled percentage for templates. Comparatively, the co-transcriptional capping process combined with affinity purification utilized a single oligo-dT step. Although one oligo-dT purification still left the mRNA purity between highest and lowest supercoiled percentage group about 10% difference, it indeed exhibited a significant improvement in mRNA purity in all groups.

Impact of supercoiled DNA percentage on mRNA IVT yield and oligo-dT recovery yield

While mRNA *in vitro* transcription yield may not be considered a critical quality attribute (CQA), it remains a crucial factor for budgeting the manufacturing. As shown in Figure 4A, lower supercoiled percentages resulted in reduced mRNA IVT yields for both the FLuc and COVID mRNAs. Although the exact reasons behind this reduction are not explicitly elucidated in this study, it is likely attributed to the production of a higher number of mRNA fragments associated with lower supercoiled DNA percentages. On one hand, LiCl precipitation may lead to the loss of smaller mRNA fragments,[20] which are preferably produced from lower supercoiled plasmids. On the other hand, precipitated mRNA fragments may weigh less than intact mRNA, assuming that the transcription start is the rate-limiting step.[21]

In addition to IVT yield, the recovery yield of oligo-dT is also an important consideration. It is reasonable to expect that mRNA with lower purity would exhibit decreased recovery yields, as fragmented mRNA lacking a sufficient poly(A) tail would not bind effectively to oligo-dT. As demonstrated in Figure 4B, the oligo-dT recovery yield reduced with decreasing supercoiled percentage. This observation is consistent with the trend observed in mRNA purity as shown in Figures 3E and 3F. Furthermore, fractions collected during the loading step were compared to the main fractions collected during the elution step using CE, as shown in Figures S9 and S7. It is evident that only minimal amounts of intact mRNA were found in the unbound fractions, emphasizing the necessity of oligo-dT chromatography as a crucial purification process for mRNA with insufficient purity.

Impact of supercoiled DNA percentage on mRNA Poly(A) tail distribution

mRNA poly(A) tail length might be influenced by plasmid nicks occurring at the poly(A) region. Oligo-dT chromatography has the

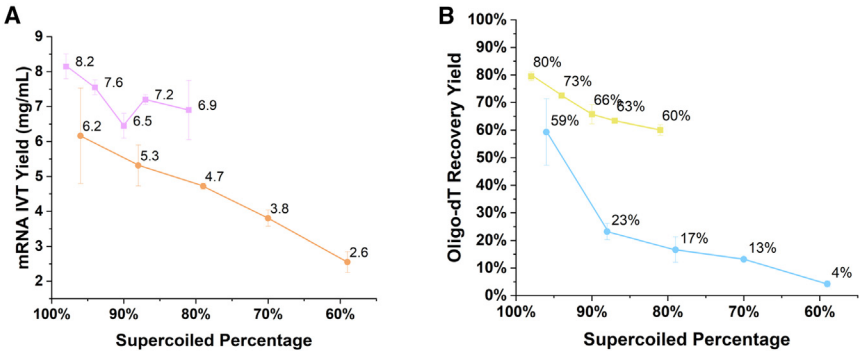

Figure 4. Comparison of mRNA IVT yield and oligo-dT recovery yield

(A) Change of mRNA IVT yield (purple is for FLuc mRNA and orange is for COVID mRNA). (B) Change of oligo-dT recovery yield (yellow is for FLuc mRNA and blue is for COVID mRNA). Data are represented as mean ± SD.

potential to retain mRNA with a desired poly(A) tail length, thereby shifting the poly(A) distribution toward the target length. T7 RNA polymerase, responsible for run-off transcription, may occasionally miss or add extra nucleotides at the end, resulting in a distribution of poly(A) tail lengths rather than a specific length.[22,23] In this study, liquid chromatography-mass spectrometry (LCMS) was employed to compare the poly(A) distributions at a high-resolution level.[24] Ribonuclease T1 was used in this experiment, and it specifically degraded single-stranded RNA and cleaved the phosphodiester bond between the 3′-guanylic residue and the 5′-OH residue of adjacent nucleotides, thus the poly(A) tracts contained a few cytidines and uridines as well as one guanidine. Based on the theoretical molecular weight of poly(A) tracts, poly A tail distribution can be detected on LCMS.

Surprisingly, no significant differences in poly(A) distributions were observed when comparing high and low supercoiled DNA percentages. Both FLuc mRNA, with a continuous 100A tail (Figure 1A), and COVID mRNA, with a segmented poly(A) tail consisting of 30A connected to 70A (Figure 1A) through a small non-A linker,[25] exhibited poly(A) distributions that matched the target poly(A) tail length. Treatment with ribonuclease T1 led to the separation of the segmented poly(A) linker into 30A and 70A sections, while the continuous 100A tail remained undigested. As illustrated in Figures 5 and S10, there were no evident shifts in poly(A) distributions for either mRNA, irrespective of the supercoiled DNA percentages and purification processes tested in our study. This suggests that supercoiled DNA percentages did not compromise mRNA poly(A) distribution.

This finding might contradict our initial hypothesis, but it can be explained by considering that the poly(A) tail region on the supercoiled plasmid may not have been damaged. The presence of a long adenine-thymine track within the plasmid may lack constraints[26] and remain intact during the heating process. Additionally, although low supercoiled DNA percentages resulted in mRNA of reduced purity, transcribed RNA sequences lacking poly(A) tails were effectively digested by ribonuclease T1, ensuring that they did not influence the analysis of poly(A) tail distribution.

Influence of supercoiled DNA percentage on dsRNA content

dsRNA is naturally formed as a byproduct of the IVT reaction and possesses immunostimulatory properties.[27] Quantification of dsRNA was conducted using an ELISA method. In Figures 6A and 6B, the results showed almost no impact on dsRNA content for FLuc mRNA but a dramatic increase for COVID mRNA along with the decline of supercoiled DNA percentage. The mechanisms underlying dsRNA formation during IVT reaction are diverse,[15,16] and it remains unclear why and how the supercoiled DNA percentage might affect the dsRNA contents differently in this study. However, oligo-dT chromatography seems to enrich dsRNA content in the case of COVID mRNA. It is possible that the self-templated 3′ extended dsRNA[28] was concentrated due to the increase of full-length mRNA percentage by oligo-dT chromatography.

This observation warrants further investigation to understand the relationship between supercoiled DNA percentage and dsRNA content in mRNA product. Additional studies are required to elucidate the specific mechanisms through which supercoiled DNA influences the generation or reduction of dsRNA during mRNA production.

Impact of supercoiled DNA percentage on capping efficiency

The presence of a natural Cap1 structure is crucial for efficient protein expression and is commonly incorporated in mRNA design. Both enzymatic capping and co-transcriptional capping methods are widely utilized in mRNA manufacturing processes. Interestingly, the capping efficiency for both methods did not appear to be affected by the supercoiled DNA percentage, as depicted in Figures 7A and 7B. Instead, a decrease in supercoiled DNA percentage primarily affected mRNA yield and purity rather than capping efficiency. This suggests that transcribed mRNA, whether full-length or missing 3′ sequence (5′ intact), can be successfully capped and detected in both capping methods.

Comparing Figures 7A with 7B, it becomes evident that the purification process plays a significant role in enzymatic capping. Specifically, the LiCl precipitation process demonstrated approximately 90% capping efficiency, while the oligo-dT purification process exhibited around 99% capping efficiency. It is plausible that the oligo-dT purification step removed impurities that may have hindered enzymatic capping. In contrast, co-transcriptional capping with a Cap1 analogue consistently provided similar capping efficiency regardless of the purification method, as capping is completed at the outset of the IVT reaction.

However, it is important to note that the capping efficiency testing described above was limited to measuring mRNA sequences

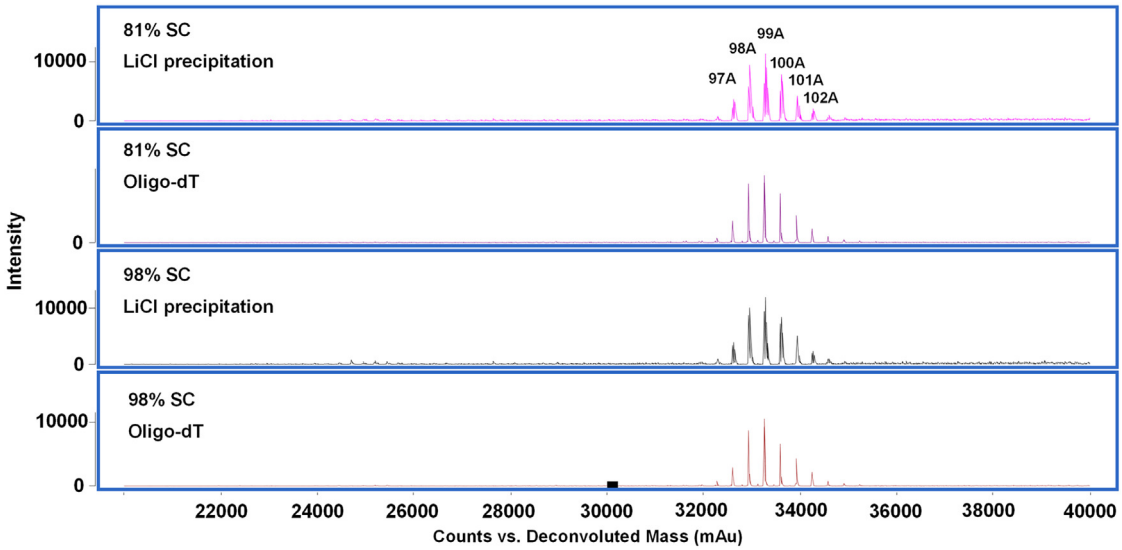

Figure 5. Comparison of poly(A) distribution of FLuc mRNA generated from different supercoiled DNA and purification processes

The poly(A) tracts contain U, C, and G due to the digestion mechanism of ribonuclease T1, and non-A nucleotides are intentionally omitted to highlight the numbers of A.

with intact 5′ ends of approximately 10–20 nt.[29] Consequently, degraded mRNA sequences lacking the 5′ end were not accounted for in the analysis. Such degraded mRNA sequences are unlikely to be caused by broken DNA templates, as the IVT reaction commences with the promoter followed by the 5′ end. Instead, these degraded sequences may arise during IVT, enzymatic capping, or subsequent downstream processes when formed mRNA strands degrade.

Overall, while the precise determination of successfully capped mRNA sequences over the total number of RNA molecules is challenging, the current results do not establish a correlation between capping efficiency and supercoiled DNA percentage. Further investigations are necessary to gain a more comprehensive understanding of the factors influencing capping efficiency and their potential relationship with supercoiled DNA content.

Impact of supercoiled DNA percentage on mRNA potency

As a drug substance, the protein expression of this mRNA as well as the functionality of target protein is defined as potency, which can be measured by an *in vitro* or *in vivo* assay. Here, we employed cell-based protein expression assay to quantify the mRNA potency. Dose-dependent FLuc protein expression with mRNA from plasmids with varying supercoiled DNA percentages are presented in Figures 8A and 8B. Given the direct influence of supercoiled DNA percentage on FLuc mRNA purity, as observed previously in our study (Figures 2 and 3), the correlation between supercoiled DNA percentage and protein expression at specific FLuc mRNA dose was also established, as depicted in Figures 8C and 8D. Here, luminous intensity of FLuc is an indicator to represent the functional FLuc protein expression in the cell.

In all FLuc mRNA dosing groups, we observed clear patterns that FLuc mRNA produced from higher supercoiled DNA percentage templates displayed much higher luminous intensity in cells. Note that the mRNA purity from 98% supercoiled DNA template was 86% and decreased to 62% from 81% supercoiled DNA template when LiCl precipitation purification was performed (Figure 3E). This 24% purity difference became almost 3-fold difference on the protein expression level resulting in cell potency. Similar cell-based potency results were also found in earlier reports.[16] On the other hand, mRNAs purified by oligo-dT reduced the impact of supercoiled percentage from DNA template and showed overall higher purity compared with mRNAs purified by LiCl precipitation, given the same IVT and storage conditions were used. Indeed, at any given dose, cells transfected with FLuc mRNAs purified by oligo-dT showed higher luminous intensity than those cells transfected with mRNAs purified by LiCl precipitation. Although the mRNA purity varied little after affinity purification, it was still notable on the potency level. Further optimizations on mRNA purity analysis or protein expression assay may be needed.

These findings highlight the importance of optimizing supercoiled DNA percentage and employing affinity purification methods to minimize the negative effects of low supercoiled DNA percentages on protein expression. It suggests that the selection of appropriate manufacturing processes and purification strategies can help improve protein expression levels and ensure consistent and reliable results.[16,30]

DISCUSSION

The purity of mRNA is a crucial attribute that directly influences its functionality and safety. In this study, we observed a clear correlation

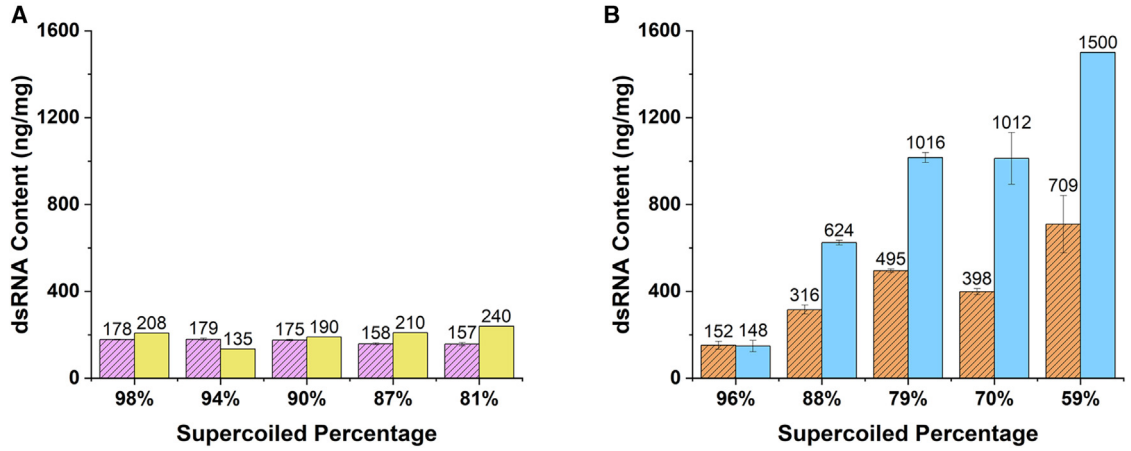

Figure 6. Comparison of dsRNA content generated from non-affinity and affinity process

(A) FLuc mRNA dsRNA content change with supercoiled DNA percentage (purple is FLuc mRNA manufactured by LiCl precipitation and yellow is FLuc mRNA manufactured by oligo-dT chromatography). (B) COVID mRNA dsRNA content change with supercoiled DNA percentage (orange is COVID mRNA manufactured by LiCl precipitation and blue is COVID mRNA manufactured by oligo-dT chromatography. Note: at 59% supercoiled percentage, the dsRNA content is beyond 1,500 ng/mg, the upper quantitative limit). Data are represented as mean ± SD.

between lower supercoiled DNA percentages in plasmid DNA and reduced mRNA purity. Heat-induced nicks in the supercoiled plasmid DNA template ultimately led to the generation of mRNA fragments, resulting in broader shoulder peaks observed in CE results. A lower supercoiled DNA percentage or higher OC percentage signifies the presence of more broken points on the DNA template. If some of the broken points occur on the antisense strand within the mRNA coding region, incomplete RNA fragments directly after IVT are inevitable (Figure 1C). These fragmented impurities further affected protein expression from mRNA and dramatically reduced the potency. In this respect, it is pivotal to maintain a high degree of homogeneity of the DNA template to set for high mRNA purity. Currently, it is still challenging to analyze and identify the nicks on the linear double-stranded DNA template, but the nicks on plasmid DNA (pDNA) resulting in the pDNA in OC forms can be well separated from supercoiled forms on HPLC.[31] This underscores the rationale behind setting the supercoiled DNA percentage as a key IPC for the manufacturing of linear DNA templates. It is essential to ensure that the supercoiled DNA percentage falls within the specified range to guarantee the successful production of linear DNA template and further mRNA drug substance.

The implementation of oligo-dT chromatography proved effective in removing degraded mRNA fragments lacking sufficient poly(A) tails, thereby enhancing mRNA purity. Notably, the affinity purification process using oligo-dT exhibited superior performance in improving mRNA purity compared to the non-affinity purification method of LiCl precipitation, as expected. However, this improvement comes at the cost of reduced yield and the use of expensive oligo-dT resins or monolith. Although mRNA yield is not a CQA, it holds strategic importance for CMC team of each mRNA pipeline, especially in large-scale productions for clinical trials and commercialization. Therefore, striking a balance between the supercoiled DNA percentage as an IPC and the manufacturing process of linear DNA templates and mRNA is essential. More specific, setting a tighter range for supercoiled DNA percentage requires a robust linear DNA manufacturing process, potentially involving additional chromatography steps, and leading to lower yield of DNA template. However, this approach allows for higher mRNA yield, improved purity, better potency and reduced risks of failure of mRNA manufacturing. As an extreme example, a linear DNA template with sufficiently high uniformity might save the use of oligo-dT chromatography in mRNA production, assuming optimal IVT conditions and proper storage are used. On the other hand, a wider range of supercoiled DNA percentage shifts the burdens from DNA template manufacturing to the more costly mRNA manufacturing process. Thus, the determination of the target IPC range should consider various factors encompassing DNA and mRNA manufacturing, such as release specifications, cost considerations, yield optimization, and process robustness.

Ideally, a regulatory-guided supercoiled DNA percentage range as the target IPC for plasmid production is preferred, but the release specifications of a specific mRNA drug candidate should also be taken into consideration when determining the range. Additionally, the supercoiled DNA percentage range should be tailored to the mRNA sequences and lengths, as demonstrated by the differing mRNA purity results from 80% supercoiled FLuc and COVID plasmids (Figures 3A and 3C), as well as the conflicting performance of dsRNA contents between FLuc mRNA and COVID mRNA (Figure 6). For example, if the mRNA purity release specification is set as 80% on the current CE method and affinity process is used in mRNA manufacturing in the two examples provided herein, it appears that quite a wide range of supercoiled DNA percentages may be accepted

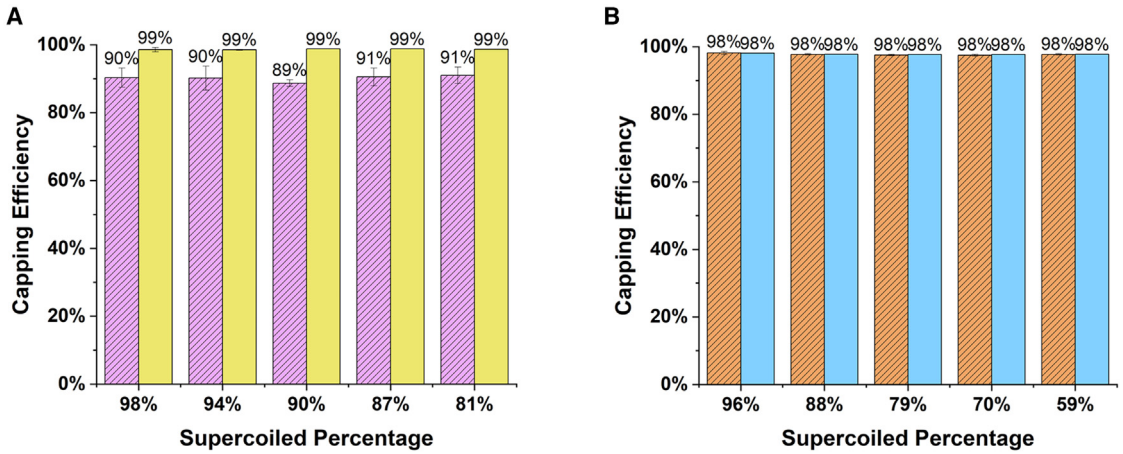

Figure 7. Summary of 5′ capping efficiency from different mRNA manufacturing processes

(A) FLuc mRNA capping efficiency change with supercoiled DNA percentage (purple is FLuc mRNA manufactured by LiCl precipitation and yellow is FLuc mRNA manufactured by oligo-dT chromatography). (B) COVID mRNA capping efficiency change with supercoiled DNA percentage (orange is COVID mRNA manufactured by LiCl precipitation and blue is COVID mRNA manufactured by oligo-dT chromatography). Data are represented as mean ± SD.

(Figures 3E and 3F). However, when considering dsRNA content and assuming 300 ng/mg is the release specification, it narrows the supercoiled DNA percentage range dramatically for COVID DNA template but there are almost no restraints on supercoiled DNA percentage toward FLuc DNA template. These hypothetical examples again highlight the significance of customizing the range of supercoiled DNA percentages for different mRNA pipelines. Overall, it seems reasonable to suggest a preferably >80% supercoiled DNA percentage to control the plasmid quality for early-phase studies, with the condition that affinity purification is employed in the mRNA manufacturing process. This suggested supercoiled percentage is consistent with *Guidance for Industry: Considerations for Plasmid DNA Vaccines for Infectious Disease Indications* by the US Food and Drug Administration (FDA),[32] despite the different purpose of plasmid DNA. It is also reasonable to gradually tighten the supercoiled DNA percentage control moving toward late-phase studies in the considerations of safety and efficacy observations.

Our study focused on the DNA template derived from *Escherichia coli* fermentation, which is currently the mainstream process for producing the DNA template used in mRNA manufacturing. However, there is a growing interest in utilizing cell-free DNA production methods to address unmet needs in mRNA therapeutics and synthetic biology.[33–35] The adoption of cell-free DNA systems for mRNA production offers a more streamlined and controlled approach, presenting various advantages in terms of simplicity, control, speed, scalability, and flexibility. It is important to note that, during cell-free DNA production, the circular DNA step may be omitted. Consequently, stringent control measures are necessary to ensure the integrity of the linear DNA template for mRNA synthesis. We believe that these advantageous characteristics render cell-free DNA systems an invaluable tool for advancing mRNA-based vaccines, therapeutics, and other applications.

In conclusion, we propose that the supercoiled DNA percentage should be considered as a key IPC parameter during linear DNA template manufacturing. By carefully establishing the IPC range for plasmid DNA and taking into account multiple aspects in the CMC work of DNA template and mRNA, we can achieve the successful development of high-quality mRNA drug substances. We hope the valuable insights gained from this study can benefit the process development of mRNA drug substances in the pharmaceutical industry to ensure the consistent and reliable quality of mRNA-based vaccines and therapeutics.

MATERIALS AND METHODS

Plasmids and DNA template generation

Plasmids were first produced at 3 L scale *E. coli* fermentation in a 5 L glass bioreactor at 37°C for 20 h followed by alkaline lysis and purification through multiple chromatography steps.[36] In order to generate desired supercoiled percentage DNA template, plasmid samples were treated with heat to generate non-supercoiled formats and evaluated across 24 h. Three temperatures (50°C, 55°C, and 60°C) were applied respectively and samples were collected hourly then analyzed on a 0.6% agarose gel (100 V, 60 min, 1× Tris-Acetate-EDTA (TAE) buffer, pre-stained with GelRed) to estimate the supercoiled percentage (Figure S11). Through analysis, combinations of temperature and time were found to obtain plasmid with a certain target supercoiled percentage through heat treatments (Tables S1 and S2). Later, 2 mg of each purified plasmid DNA dissolved in MilliQ water was treated accordingly, then quantified by HPLC to confirm the supercoiled percentage (Tables S1 and S2). Linear DNA templates were generated by incubating plasmids with corresponding restriction enzyme (EcoRI for FLuc plasmid and XbaI for COVID plasmid, enzyme: SC plasmid = 2 U: 1 μg; restriction enzymes were supplied by New England Biolabs) at 37°C for 5 h. After linearization,

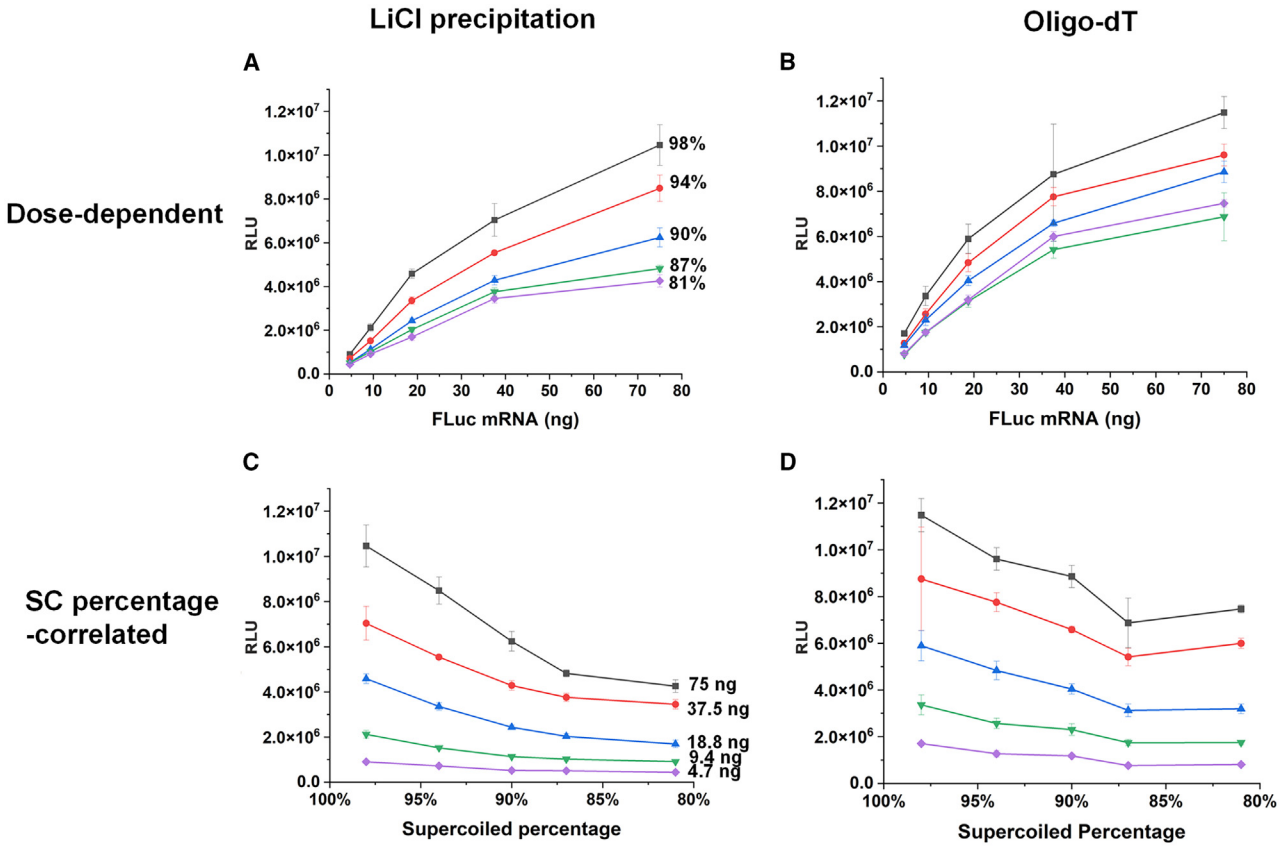

Figure 8. FLuc mRNA potency

(A) Dose-dependent potency for FLuc mRNA generated from DNA template with different SC percentage and purified by LiCl precipitation. (B) Dose-dependent potency for FLuc mRNA generated from DNA template with different SC percentage and purified by oligo-dT chromatography (black line is 98% SC, red line is 94% SC, blue line is 90% SC, green line is 87% SC, and purple line is 81% SC). (C) Correlation of FLuc mRNA potency and supercoiled DNA percentage; mRNA was purified by LiCl precipitation. (D) Correlation of FLuc mRNA potency and supercoiled DNA percentage; mRNA was purified by oligo-dT chromatography (black line is 75 ng, red line is 37.5 ng, blue line is 18.8 ng, green line is 9.4 ng, and purple line is 4.7 ng). Data are represented as mean ± SD.

the linear DNA templates were purified by ethanol precipitation and redissolved in 20 mM Tris buffer (pH 7.5).

HPLC of supercoiled DNA

The HPLC method was adapted from an earlier report.[31] The 40-ng/μL supercoiled DNA samples were injected into the column at 25°C. Buffer A was 20 mM Tris and 0.5 M NaCl; buffer B was 20 mM Tris and 1 M NaCl. Sample was separated with increasing percentage of buffer B at total flow rate of 0.5 mL/min. UV absorbance at 260 nm was used to monitor samples. Thermo Scientific DNAPac column was applied for separation. HPLC analysis of supercoiled DNA was performed on Agilent HPLC 1260 Infinity II.

qPCR of linear DNA template

Taq Pro HS Universal U + Probe Master Mix (Vazyme) was used to prepare samples, and 10-fold serial diluted samples were prepared from 50 μg/mL stock standard (unheated supercoiled sample). Different OC samples were diluted by 100-fold, 5,000-fold, and 50,000-fold for testing. In a 20-μL reaction, 1× Master Mix, 0.2 μM forward primer, 0.2 μM reverse primer, and 0.1 μM probe were mixed with testing samples (3 μL). qPCR was performed on StepOnePlus (Applied Biosystems). Heating program settings: 2-min holding stage at 50°C, 10-min holding stage at 95°C, cycling stage (40 cycles) from 15 s at 95°C to 15 s at 55°C to 3 min of holding at 72°C. Cycle threshold value was set at 0.25.

mRNA *in vitro* transcription

Here, 9 U/μL T7 RNA polymerase (Vazyme), 2 U/μL pyrophosphatase (Vazyme), 1 U/μL RNase inhibitor (Novoprotein), 8 mM of each nucleoside triphosphate (Glycogene), 50 ng/μL DNA template, 40 mM $MgCl_2$, 40 mM Tris, 10 mM DTT, and 2 mM spermidine were used in a 100 μL IVT reaction. For co-transcriptional IVT, 6.4 mM GAG cap analogue (Synthgene) was also included in the IVT reaction, and 20 mM $MgCl_2$ was used. N1-methylpseudouridine triphosphate was used instead of uridine triphosphate for all processes. The IVT reaction went on at 37°C for 2 h, followed by DNase

I (Novoprotein) digestion for 20 min. The crude IVT product was then subject to proper purification steps listed in Figure 1C. The concentration of purified mRNA was measured on Nanodrop One (Thermo Fisher Scientific).

Oligo-dT purification

Oligo-dT chromatography was performed on a 1 mL CIMmultus dT18 monolith (Sartorius BIA Separations). Equilibrium, wash, and elution buffers were prepared according to the supplier's manual. NaCl solution (4 M) was slowly added into mRNA samples to obtain a final concentration of 250 mM. After filtration, mRNA samples were loaded onto the pre-equilibrated monolith and washed with equilibrium buffer for six column volumes (CVs) followed by 5 CVs of wash buffer. Finally, 5 CVs of elution buffer was used to elute mRNA samples. UV absorbance at 260 nm was used to monitor the entire process, and elution fractions over 100 mAu were collected. Flow rate was set as 10 mL/min for the entire purification process. ÄKTA Avant (Cytiva) was used for chromatography.

Enzymatic capping

Enzymatic capping was performed according to previous literature[37] with minor modification. Vaccinia capping enzymes, 2-O-methyltransferase, S-adenosyl-methionine (SAM), and 10× buffer were provided by Novoprotein. Briefly, in a 1.3 mL capping reaction, uncapped mRNA, 1× capping buffer, GTP (0.5 mM), SAM (0.2 mM), Vaccinia capping enzyme, 2-O-methyltransferase, and RNase inhibitor (1 U/μL) were mixed together and incubated at 37°C for 60 min, followed by quenching the reaction with 10 mM EDTA.

mRNA purity measurement

The purity of mRNA was measured on Agilent Fragment Analyzer 5300 with RNA kit (15NT). Supplier's manual was followed. Briefly, 100 ng/μL mRNA samples were heated at 70°C for 2 min, then chilled on ice for 5 min. Then 2 μL of heated samples were mixed well with 22 μL of diluent, followed by transferring onto an Eppendorf 96-well plate. A 6,000-nt RNA ladder from the kit was used as the marker to estimate size of mRNA. Pre-set RNA method was used for separation. ProSize 2.0 software was used to process the raw data. Two vertical lines were drawn through inflection points of the main peak for integration (dot lines in Figures S5–S8).

Poly(A) distribution measurement

Poly(A) tail distribution measurement was adapted from a previous study[24] with minor modifications. mRNA samples were first digested by RNase T1 to acquire poly(A) tail. Briefly, 50 μg of mRNA in 44 μL of water, 1 μL of RNase T1 (Thermo Fisher Scientific), and 5 μL of 1 M NH_4OAc were mixed in an Eppendorf tube. The resulting mixture was vortexed briefly and kept at 37°C with shaking at 1,500 rpm for 1 h. The solution after RNase T1 digestion was immediately transferred to a 2°C–8°C refrigerator and allowed to stand for 3–5 min. The cooled solution was briefly centrifuged, followed by a brief vortex, and transferred to the HPLC vial for injection. The digested solution was then injected to a 6545XT Q-TOF mass spectrometer coupled to an Agilent 1290 Infinity II LC system.

dsRNA quantification by ELISA

CatPure^{TM} dsRNA (N1mpU) reference standard used in this assay was supplied by CATUG Biotechnology (catalog # CT40000) and the ELISA kit was ordered from Vazyme. Supplier's manual was followed. Briefly, 5 μL of standard dsRNA (adjusted to 300 ng/mL) was diluted with 995 μL of sample diluent, then standard samples were prepared by 2-fold dilution. One-hundred microliters of samples were added into each well of the pre-coated 96-well plate, and the sealed plate was incubated at 37°C for 1 h, then the solution was discarded. Plate was washed with 1× wash buffer (300 μL) for 30 s and repeated four times. Then 1× detection antibody (100 μL) was added into each well and the sealed plate was incubated at 37°C for 1 h, followed by wash step, and then 1× enzyme-labeled reagent (100 μL) was added into each well and the sealed plate was incubated at 37°C for 1 h, followed by wash. Finally, TMB substrate (100 μL) was added into each well and the sealed plate was incubated at 37°C for 15 min. Then 50 μL of stop solution was added into each well and mixed well. Spectramax iD5 (Molecular Devices) was used to measure the optical density (OD) value per well at a single wavelength of 450 nm.

Capping efficiency measurement

Capping efficiency measurement was adapted from previous literature[29] with minor modifications. Briefly, a short DNA-RNA chimera complementary to 5′ UTR sequence of mRNA was synthesized to guide RNase H cleavage at 5′ UTR. The enzymatic reaction system consisted of 30 μg of purified mRNA, 3 μL of 10× reaction buffer (500 mM Tris-HCl, pH 8, 750 mM KCl, and 30 mM $MgCl_2$), 2 μL of thermostable RNase H (Novoprotein), and 2 μL of synthesized guide at 0.1 M concentration. The mixture was incubated in thermomixer at 65°C for 15 min and cooled immediately in a 2°C–8°C refrigerator for 5 min, followed by addition of 5 μL of 0.25 M EDTA for quenching. The digested sample was then injected into 6545XT Q-TOF mass spectrometer coupled to an Agilent 1290 Infinity II LC system.

FLuc mRNA potency

HeLa cells were used for FLuc mRNA expression study. MEM/EBSS (Cytiva), Opti-MEM and fetal bovine serum (Gibco), Lipofectamine MessengerMAX (Thermo Fisher Scientific), and One-Lite Luciferase Assay Substrate (Promega) were employed for potency assay. CatPure^{TM} FLuc mRNA from CATUG Biotechnology (catalog # CT072) was used as positive control for potency assay. About 1×10^4 cells were seeded in 96-well plate and incubated at 37°C with 5% CO_2 for 18 h. Transfection was done according to supplier's manual and cells were incubated for 24 h post transfection. One-Lite Luciferase Assay Substrate (50 μL) was added to cells and held for 7 min before reading luminescence on Spectramax iD5 (Molecular Devices).

DATA AND CODE AVAILABILITY

Supplemental information is available online. Raw data are available upon request.

SUPPLEMENTAL INFORMATION

Supplemental information can be found online at https://doi.org/10.1016/j.omtn.2024.102223.

ACKNOWLEDGMENTS

The authors would like to send appreciation to Ms. Simin Tao for illustrative figures in this paper.

AUTHOR CONTRIBUTIONS

X.P. and L.J. designed the experiment and wrote the manuscript. Y.T., X.L., W.Z., W.Y., X.X., W.W., J.J., J.X., K.H., M.X., and M.L. performed experiments. M.S. revised the manuscript.

DECLARATION OF INTERESTS

All authors are employees of CATUG Biotechnology and may be shareholders of CATUG Biotechnology.

REFERENCES

1. Barbier, A.J., Jiang, A.Y., Zhang, P., Wooster, R., and Anderson, D.G. (2022). The clinical progress of mRNA vaccines and immunotherapies. Nat. Biotechnol. *40*, 840–854.
2. Lorentzen, C.L., Haanen, J.B., Met, Ö., and Svane, I.M. (2022). Clinical advances and ongoing trials on mRNA vaccines for cancer treatment. Lancet Oncol. *23*, e450–e458.
3. Rosa, S.S., Prazeres, D.M.F., Azevedo, A.M., and Marques, M.P.C. (2021). mRNA vaccines manufacturing: Challenges and bottlenecks. Vaccine *39*, 2190–2200.
4. Whitley, J., Zwolinski, C., Denis, C., Maughan, M., Hayles, L., Clarke, D., Snare, M., Liao, H., Chiou, S., Marmura, T., et al. (2022). Development of mRNA manufacturing for vaccines and therapeutics: mRNA platform requirements and development of a scalable production process to support early phase clinical trials. Transl. Res. *242*, 38–55.
5. Kang, D.D., Li, H., and Dong, Y. (2023). Advancements of *in vitro* transcribed mRNA (IVT mRNA) to enable translation into the clinics. Adv. Drug Deliv. Rev. *199*, 114961.
6. Fuchs, A.-L., Neu, A., and Sprangers, R. (2016). A general method for rapid and cost-efficient large-scale production of 5' capped RNA. RNA *22*, 1454–1466.
7. Jemielity, J., Fowler, T., Zuberek, J., Stepinski, J., Lewdorowicz, M., Niedzwiecka, A., Stolarski, R., Darzynkiewicz, E., and Rhoads, R.E. (2003). Novel "anti-reverse" cap analogs with superior translational properties. RNA *9*, 1108–1122.
8. Henderson, J.M., Ujita, A., Hill, E., Yousif-Rosales, S., Smith, C., Ko, N., McReynolds, T., Cabral, C.R., Escamilla-Powers, J.R., and Houston, M.E. (2021). Cap 1 Messenger RNA Synthesis with Co-transcriptional CleanCap® Analog by *In Vitro* Transcription. Curr. Protoc. *1*, e39.
9. Walker, S.E., and Lorsch, J. (2013). RNA purification–precipitation methods. Methods Enzymol. *530*, 337–343.
10. Green, M.R., and Sambrook, J. (2019). Isolation of Poly(A)+ Messenger RNA Using Magnetic Oligo(dT) Beads. Cold Spring Harb. Protoc. *2019*. pdb.prot101733.
11. Mencin, N., Štepec, D., Margon, A., Vidič, J., Dolenc, D., Simčič, T., Rotar, S., Sekirnik, R., Štrancar, A., and Černigoj, U. (2023). Development and scale-up of Oligo-dT monolithic chromatographic column for mRNA capture through understanding of base-pairing interactions. Sep. Purif. Technol. *304*, 122320.
12. Webb, C., Ip, S., Bathula, N.V., Popova, P., Soriano, S.K.V., Ly, H.H., Eryilmaz, B., Nguyen Huu, V.A., Broadhead, R., Rabel, M., et al. (2022). Current Status and Future Perspectives on MRNA Drug Manufacturing. Mol. Pharm. *19*, 1047–1058.
13. Agrawal, P., Wilkstein, K., Guinn, E., Mason, M., Serrano Martinez, C.I., and Saylae, J. (2023). A Review of Tangential Flow Filtration: Process Development and Applications in the Pharmaceutical Industry. Org. Process Res. Dev. *27*, 571–591.
14. Daniel, S., Kis, Z., Kontoravdi, C., and Shah, N. (2022). Quality by Design for enabling RNA platform production processes. Trends Biotechnol. *40*, 1213–1228.
15. Wu, M.Z., Asahara, H., Tzertzinis, G., and Roy, B. (2020). Synthesis of low immunogenicity RNA with high-temperature *in vitro* transcription. RNA *26*, 345–360.
16. Piao, X., Yadav, V., Wang, E., Chang, W., Tau, L., Lindenmuth, B.E., and Wang, S.X. (2022). Double-stranded RNA reduction by chaotropic agents during *in vitro* transcription of messenger RNA. Mol. Ther. Nucleic Acids *29*, 618–624.
17. Wienert, B., Shin, J., Zelin, E., Pestal, K., and Corn, J.E. (2018). In vitro–transcribed guide RNAs trigger an innate immune response via the RIG-I pathway. PLoS Biol. *16*, e2005840.
18. Levy, M.S., Lotfian, P., O'Kennedy, R., Lo-Yim, M.Y., and Shamlou, P.A. (2000). Quantitation of supercoiled circular content in plasmid DNA solutions using a fluorescence-based method. Nucleic Acids Res. *28*, E57.
19. Neil, A.J., Belotserkovskii, B.P., and Hanawalt, P.C. (2012). Transcription blockage by bulky end termini at single-strand breaks in the DNA template: differential effects of 5' and 3' adducts. Biochemistry *51*, 8964–8970.
20. Nilsen, T.W. (2012). Selective precipitation of large RNAs. Cold Spring Harb. Protoc. *2012*, pdb.prot072322.
21. Anand, V.S., and Patel, S.S. (2006). Transient state kinetics of transcription elongation by T7 RNA polymerase. J. Biol. Chem. *281*, 35677–35685.
22. Gau, B.C., Dawdy, A.W., Wang, H.L., Bare, B., Castaneda, C.H., Friese, O.V., Thompson, M.S., Lerch, T.F., Cirelli, D.J., and Rouse, J.C. (2023). Oligonucleotide mapping via mass spectrometry to enable comprehensive primary structure characterization of an mRNA vaccine against SARS-CoV-2. Sci. Rep. *13*, 9038.
23. Koscielniak, D., Wons, E., Wilkowska, K., and Sektas, M. (2018). Non-programmed transcriptional frameshifting is common and highly RNA polymerase type-dependent. Microb. Cell Fact. *17*, 184.
24. Beverly, M., Hagen, C., and Slack, O. (2018). Poly A tail length analysis of *in vitro* transcribed mRNA by LC-MS. Anal. Bioanal. Chem. *410*, 1667–1677.
25. Trepotec, Z., Geiger, J., Plank, C., Aneja, M.K., and Rudolph, C. (2019). Segmented poly(A) tails significantly reduce recombination of plasmid DNA without affecting mRNA translation efficiency or half-life. RNA *25*, 507–518.
26. Bowater, R., Aboul-ela, F., and Lilley, D.M. (1991). Large-scale stable opening of supercoiled DNA in response to temperature and supercoiling in (A + T)-rich regions that promote low-salt cruciform extrusion. Biochemistry *30*, 11495–11506.
27. Mu, X., and Hur, S. (2021). Immunogenicity of In Vitro-Transcribed RNA. Acc. Chem. Res. *54*, 4012–4023.
28. Gholamalipour, Y., Karunanayake Mudiyanselage, A., and Martin, C.T. (2018). 3' end additions by T7 RNA polymerase are RNA self-templated, distributive and diverse in character-RNA-Seq analyses. Nucleic Acids Res. *46*, 9253–9263.
29. Beverly, M., Dell, A., Parmar, P., and Houghton, L. (2016). Label-free analysis of mRNA capping efficiency using RNase H probes and LC-MS. Anal. Bioanal. Chem. *408*, 5021–5030.
30. Nelson, J., Sorensen, E.W., Mintri, S., Rabideau, A.E., Zheng, W., Besin, G., Khatwani, N., Su, S.V., Miracco, E.J., Issa, W.J., et al. (2020). Impact of mRNA chemistry and manufacturing process on innate immune activation. Sci. Adv. *6*, eaaz6893.
31. Molloy, M.J., Hall, V.S., Bailey, S.I., Griffin, K.J., Faulkner, J., and Uden, M. (2004). Effective and robust plasmid topology analysis and the subsequent characterization of the plasmid isoforms thereby observed. Nucleic Acids Res. *32*, e129.
32. U.S. Food and Drug Administration (2007). Guidance for Industry: Considerations for Plasmid DNA Vaccines for Infectious Disease Indications. https://www.fda.gov/regulatory-information/search-fda-guidance-documents/considerations-plasmid-dna-vaccines-infectious-disease-indications.
33. Yabuki, T., Motoda, Y., Hanada, K., Nunokawa, E., Saito, M., Seki, E., Inoue, M., Kigawa, T., and Yokoyama, S. (2007). A robust two-step PCR method of template DNA production for high-throughput cell-free protein synthesis. J. Struct. Funct. Genom. *8*, 173–191.

34. Adie, T., Orefo, I., Kysh, D., Kondas, K., Thapa, S., Extance, J., Duncan, T., and Rothwell, P.J. (2022). dbDNA™: An advanced platform for genetic medicines. Drug Discov. Today *27*, 374–377.

35. de Mey, W., De Schrijver, P., Autaers, D., Pfitzer, L., Fant, B., Locy, H., Esprit, A., Lybaert, L., Bogaert, C., Verdonck, M., et al. (2022). A synthetic DNA template for fast manufacturing of versatile single epitope mRNA. Mol. Ther. Nucleic Acids *29*, 943–954.

36. Lemmens, R., Olsson, U., Nyhammar, T., and Stadler, J. (2003). Supercoiled plasmid DNA: selective purification by thiophilic/aromatic adsorption. J. Chromatogr. B *784*, 291–300.

37. McKenzie, R.E., Minnell, J.J., Ganley, M., Painter, G.F., and Draper, S.L. (2023). mRNA Synthesis and Encapsulation in Ionizable Lipid Nanoparticles. Curr. Protoc. *3*, e898.